

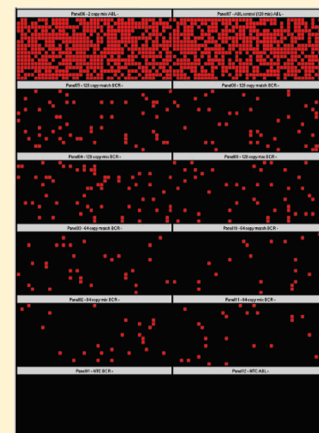
Evaluation of Digital PCR for Absolute DNA Quantification

Rebecca Sanders, Jim F. Huggett,* Claire A. Bushell, Simon Cowen, Daniel J. Scott, and Carole A. Foy

LGC, Queens Road, Teddington, Middlesex TW11 0LY

Supporting Information

ABSTRACT: The emerging technique of microfluidic digital PCR (dPCR) offers a unique approach to real-time quantitative PCR for measuring nucleic acids that may be particularly suited for low-level detection. In this study, we evaluated the quantitative capabilities of dPCR when measuring small amounts (<200 copies) of DNA and investigated parameters influencing technical performance. We used various DNA templates, matrixes, and assays to evaluate the precision, sensitivity and reproducibility of dPCR, and demonstrate that this technique can be highly reproducible when performed at different times and when different primer sets are targeting the same molecule. dPCR exhibited good analytical sensitivity and was reproducible outside the range recommended by the instrument manufacturer; detecting 16 estimated targets with high precision. The inclusion of carrier had no effect on this estimated quantity, but did improve measurement precision. We report disagreement when using dPCR to measure different template types and when comparing the estimated quantities by dPCR and UV spectrophotometry. Finally, we also demonstrate that preamplification can impose a significant measurement bias. These findings provide an independent assessment of low copy molecular measurement using dPCR and underline important factors for consideration in dPCR experimental design.



Digital PCR (dPCR) transforms the exponential, analogue nature, and single molecular sensitivity of classic PCR into a linear, digital signal. Single molecules are isolated by dilution and individually amplified by PCR; each product is then analyzed separately. This is achieved by partitioning a sample prior to PCR amplification such that each reaction chamber contains 0 or ≥ 1 copies of target DNA. A Poisson correction can be factored into the result to account for chambers that contain more than one molecule, and an absolute target sequence quantity can be estimated. This partitioning of the sample also has the effect of diluting out background signal and increasing the signal-to-noise ratio of low-abundance targets. Vogelstein and Kinzler first pioneered this approach in 1999 for the detection of a mutant *ras* oncogene in the stool of patients with colorectal cancer.¹

Recent years have yielded a plethora of studies utilizing dPCR for various applications that benefit from absolute quantification. These include cancer^{1–6} and fetal diagnostics,^{7–9} single cell studies,^{10,11} GMO analysis,^{12,13} and next generation sequencing.¹⁴ dPCR has considerable potential; however, the complexities of setup make performing this approach using standard 96- or 384-well plates difficult. The emergence of microfluidics and associated development of a number of instruments capable of nanolitre reactions have circumvented these technical issues.

One such instrument is the Biomark system from Fluidigm, which uses microfluidic dPCR array chips consisting of 12 individual panels (Figure 1). Reactions (8 μL , of which 4.6 μL is distributed across the individual panel) are loaded onto the chip. Each panel consists of 765 \times 6 nL individual chambers (4.6 μL per panel), enabling 765 replicate reactions per sample and 9180 total reactions per chip (12 \times 765). For the most accurate measurement using this platform, it is recommended

that dPCR be performed at 200–700 positive chambers per 765 chamber panel.¹⁵ However, although this ideal concentration can be achieved in many situations, it is often not possible due to the fact that the sample in question is too dilute. In this study, using this platform, we evaluate the sensitivity and precision with component reproducibility of dPCR measurements to detect smaller amounts of DNA (when template DNA is ≤ 200 copies per panel). These measurements are compared with classic real-time quantitative PCR (qPCR), as the current method of choice in this field. We consider the effect of interrun variation, template type, concentration, and use of carrier on both dPCR quantification and the associated nanofluidic qPCR. We have also investigated the effect of different PCR assays on measurement and highlight discrepancies between DNA copy-number estimates derived by UV spectrophotometry and dPCR. To circumvent the issues associated with low copy-number samples, analysts may utilize preamplification. For this reason, we explored the impact of preamplification of target DNA prior to dPCR analysis. Our findings highlight key factors that should be considered when planning to use dPCR to measure small amounts of DNA and answer some rudimentary questions associated with using this technology in this way.

EXPERIMENTAL SECTION

DNA Templates. Concentrations of plasmid were estimated using Nanodrop UV spectrophotometry (Thermo Scientific,

Received: December 10, 2010

Accepted: March 29, 2011

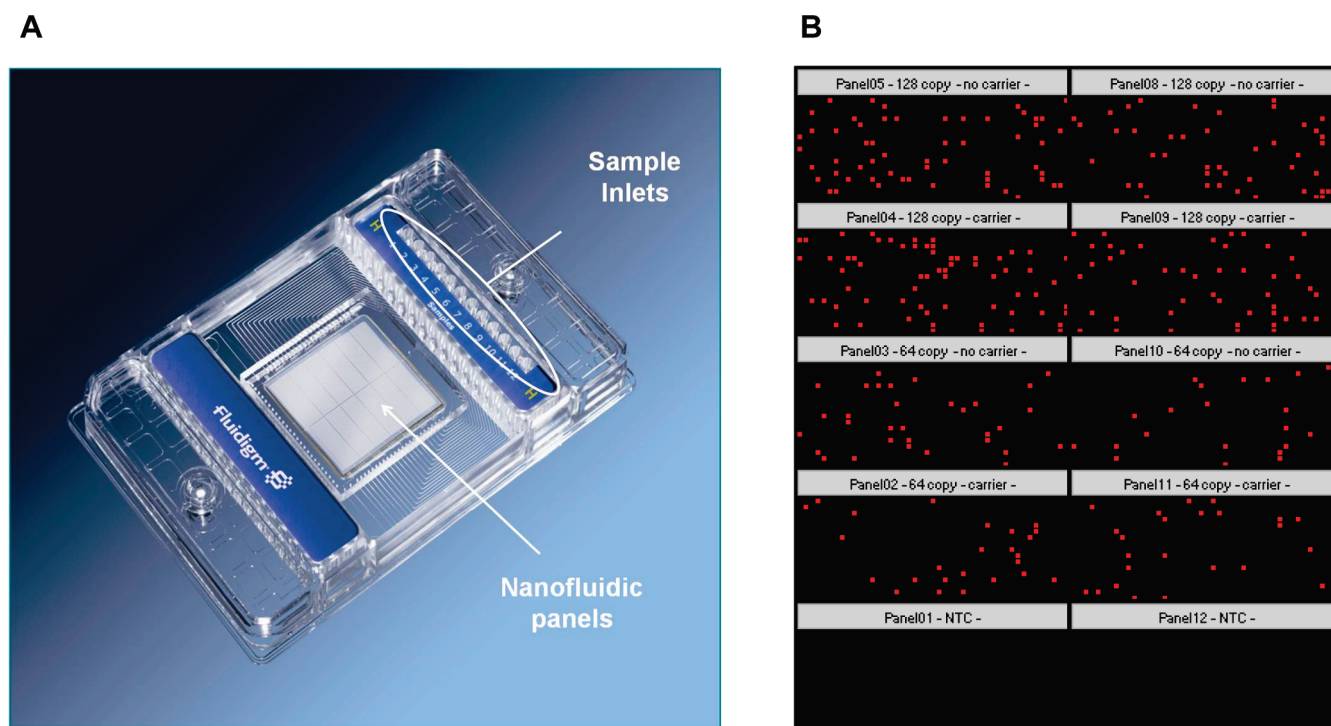


Figure 1. Microfluidic dPCR 12.765 array (Fluidigm). (A) 12.765 dPCR array chip. Master reaction mixes were loaded into 12 sample inlets and subsequently distributed within each individual panel by way of a pressure system implemented by an integrated fluidic circuit (IFC) controller, (Fluidigm). Image courtesy of Fluidigm Corporation. (B) Heat map view generated by the Biomark dPCR analysis software for low copy-number quantification experiment. The panels shown represent 10 samples: 64 and 128 copy/panel samples with and without carrier plus no template control (NTC), each in duplicate. The red spots indicate amplification has occurred; that is, target DNA is present. Black spots represent no observable amplification.

Table 1. Primer and Probe Sequences

target DNA	primer/probe sequence (5' to 3') ^a	average efficiency (%) ^b
BCR-ABL M-bcr ^{18,19}	(F) TCCGCTGACCATCAAYAAGGA	~99.6
	(R) CACTCAGACCCTGAGGCTCAA	
	(P) FAM-CCCTTCAGCGGCCAGTAGCATCTGA-TAMRA	
ABL ^{18,19}	(F) TGGAGATAACACTCTAAGCATAACTAAAGGT	~102.4
	(R) GATGTAGTTGCTTGGGACCCA	
	(P) FAM-CCATTTTTGGTTTGGGCTTCACACCATT-TAMRA	
Adh assay α , Exon 2	(F) GGTTGCTCCACCGCAGAA	~99.2
	(R) AAACATCGGTGTGACAGAGAGAAG	
	(P) FAM-AAGTTCGTATCAAGATTC-MGB	
Adh assay β , Exon 4	(F) TTGAGAGTGTGGAGAAGGAGTGA	~97.2
	(R) CGGTAAGATCGGCAACACA	
	(P) FAM-TCTTCAGCCAGGAGATC-MGB	
Adh assay δ , Exon 5	(F) TGAACCCGAAAGACCATGACA	~96.1
	(R) CCCACCATCCGTCATCTCA	
	(P) FAM-CCAATTCAACAGGTGATC-MGB	

^aF, forward primer; R, reverse primer; P, probe; MGB, minor groove binder. ^bAs determined by average of three qPCR reactions using the ABI 7900 platform.

Wilmington, DE) or provided by supplier and converted to copy number using previous methods.¹⁶ Low-bind tubes were employed throughout this study. All primer and probe sequences for dPCR were ordered from Sigma (Dorset, UK), unless otherwise stated (Table 1). Systematic LOQ (limit of quantification) was not performed for all assays; however, standard curve analysis

showed good linearity down to five copies (for detailed description of conversion between copies/ μ L and copies/panel, see the Supporting Information, Table 1).

BCR-ABL standards and assays (BCR-ABL Mbc Fusion-Quant Kit) were purchased from IPSOGEN Cancer Profiler, (Marseille, France) and diluted with and without wild type

Table 2. Sample Dilutions Analysed during Study, Derived by UV Spectrophotometry

experiment	assay	copies DNA target per reaction ^a	concn carrier ^b
low copy number quantification	BCR-ABL	~2	either 10 ng/ μ L WT cDNA carrier (assuming 100% RT efficiency) or water
		~8	
		~16	
		~32	
		~64	
		~128	
the effect of different assays and preamplification on assay bias	ADH α , β , and δ	~100	50 ng/ μ L salmon sperm DNA
the effect of DNA template types on dPCR measurement	ADH α	~57	50 ng/ μ L salmon sperm DNA

^a For detailed description of conversion between copies/ μ L and copies/panel, see Supporting Information. NTCs for every experiment resulted in no amplified signal observed. ^b Dilutions are quoted based on copies per 12.756 microfluidic dPCR panel or qPCR copies per well of a standard 96 well plate.

carrier (wild type HCC1954BL cell line lymphocyte origin, ATCC, Teddington, UK) on the basis of the copy number specified by the manufacturer (Table 2).

The pSP64 poly(A) plasmid containing the *Arabidopsis landsberg* alcohol dehydrogenase (ADH) gene fragment¹⁷ was used, either circularized or linearized with *Bgl*I; 0.5 μ g plasmid DNA was digested as per the manufacturer's instructions (New England Biolabs, Hitchin, UK). An equal quantity of the same extract of pSP64-Adh DNA was treated with a negative *Bgl*I restriction digest (omitting *Bgl*I) to yield intact pSP64-Adh plasmid. Linearization was designed to cleave the plasmid centrally within the plasmid backbone, resulting in the target sequence being located approximately equidistant from either end of the linearized molecule. Digestion was confirmed by Agilent 2100 BioAnalyzer analysis (Agilent, West Lothian, UK), performed according to the manufacturer's instructions.

For the comparison between template structures, circular and linear pSP64-Adh DNA samples (three separate digests and three separate negative digests) were diluted to ~40 copies/ μ L (57 copies/panel, see the Supporting Information for calculations) in 50 ng/ μ L constant carrier (salmon sperm DNA, Agilent). To avoid bias that may be introduced by this step, digested samples were not cleaned up. Experiments exploring the effect of different assays and preamplification on measurement bias utilized pSP64-Adh linearized template pooled from three replicate digests. These samples were subsequently subjected to QiaQuick DNA purification (Qiagen, Valencia, CA), according to the manufacturer's instructions and requantified by Nanodrop UV spectrophotometry. Sample was then diluted to ~70 copies/ μ L (100 copies/panel, see the Supporting Information for calculations) in 50 ng/ μ L constant carrier (salmon sperm DNA, Agilent). Where results were directly compared, any differences in loaded sample volume were compensated for. Data were analyzed and presented as estimated targets per reaction (copies per 12.765 dPCR panel or per well of a standard 96 well plate).

Preamplification of Target DNA. Preamplification of target DNA was performed using TaqMan Preamp Master Mix (ABI, Carlsbad, CA). All assays were optimized and assessed initially by qPCR using the Prism 7900 HT real-time PCR system (ABI) by altering primer concentration and estimating assay efficiency using standard curves. Ten microliter reactions consisted of TaqMan Preamp Master Mix (ABI), pooled sequence-specific gene assay mix (0.2 \times for each assay) and 2 μ L of DNA. Pooled sequence-specific gene assay mix was prepared in 1 \times TE,

pH 8. Preamplification was performed using the following thermocycling conditions: 95 $^{\circ}$ C for 10 min, then 14 cycles of 95 $^{\circ}$ C for 15 s and 60 $^{\circ}$ C for 4 min. As per the preamplification protocol, amplification product was diluted 1:5 in 1 \times TE, pH 8 and, from this point on, treated as neat product.

Microfluidic dPCR Analysis. Microfluidic dPCR was performed using the Biomark system with the 12.765 dPCR chip (Fluidigm, South San Francisco, CA)²⁰ (Figure 1A and B). All assays were optimized and assessed initially by qPCR as described above. Details of specific assays are outlined in Table 2. Quantification cycle (C_q) values were measured for each of the 9180 reaction chambers at a threshold setting that was consistent for the respective experimental comparisons. Eight microliter master reactions consisted of TaqMan Gene Expression Master Mix (ABI), GE Sample Loading Reagent (Fluidigm), sequence-specific gene assay (Table 1), and 2.5 μ L of DNA. All dilutions of template were made in 0.5% Tween 20 (Sigma) (Table 2). Each 8 μ L master reaction was subsequently loaded into a 12.765 dPCR chip (Fluidigm), and dPCR was performed using the following thermocycling conditions: 50 $^{\circ}$ C for 2 min, 95 $^{\circ}$ C for 10 min, then 40 cycles of 95 $^{\circ}$ C for 15 s and 60 $^{\circ}$ C for 1 min. The number of positive amplifications (counts) was used for analysis of C_q variation, whereas the number of estimated targets (based on a Poisson correction of the data to estimate the true number of copies)^{21,22} was used for quantification of target.

Real-Time Quantitative PCR Analysis. Conventional real-time quantitative PCR (qPCR) was performed using a 96-well plate format with the Prism 7900 HT real-time PCR system (ABI). Twenty-five microliter reactions consisting of TaqMan Universal Master Mix (ABI), sequence-specific gene assay (Table 1), and 1.44 μ L of DNA at various concentrations (Table 2). Samples were run in triplicate wells on each plate. PCR efficiency estimates were made using five-point, 10-fold, serially diluted standard curves (triplicate measurements performed at each point). The qPCR reaction was performed using the following parameters: 50 $^{\circ}$ C for 2 min, 95 $^{\circ}$ C for 10 min, then 50 cycles of 95 $^{\circ}$ C for 15 s and 60 $^{\circ}$ C for 1 min.

Low Copy-Number Quantification. Estimated copies per panel—2, 8, 16, 32, 64, and 128—(dPCR) or reaction (qPCR) of standard for BCR-ABL (Table 2) were investigated by both dPCR and qPCR using the BCR-ABL assay from the BCR-ABL Mbc FusionQuant Kit, with and without 2 μ g reverse-transcribed RNA carrier (wild type HCC1954BL cell line). For each copy number examined, interassay variation was investigated by performing triplicate analyses using two panels or three wells for

each carrier and no-carrier samples, with replicate experiments performed over five months. Stock DNA solutions were stored at $-20\text{ }^{\circ}\text{C}$ between experiments, and new dilutions were performed for each analysis. No template controls (NTC) were performed by adding water in place of template, and all resulted in no signal. The impact of the presence of carrier on dPCR and qPCR was assessed using mixed effects models with maximum likelihood estimation. Experiment-to-experiment variation was modeled as a random effect, while the carrier effect (present/not present) was modeled as a fixed effect. (Model summaries are given in the Supporting Information Tables 2 and 3.) The associated Cqs from each platform were also compared between replicate experiments using nonparametric Mann–Whitney U or Kruskal–Wallis tests, depending on analysis.

The Effect of Different Assays and DNA Template Types on dPCR Measurements. Three different assays targeting three different regions (GeneBank accession: M12196, position 1236–2306 bp (assay α), 1565–1630 bp (assay β) and 2158–2219 bp (assay δ)) of the *Arabidopsis thaliana* ADH gene were optimized, and efficiencies were established on the Prism 7900 HT real-time PCR platform (ABI) before being transferred to the Biomark system. All three assays were of comparable high efficiency (96–100%). Each of the three assays was assessed individually on triplicate dPCR panels of a 12.765 chip with ~ 100 copies/panel of linear pSP64-Adh DNA, along with relevant controls. In addition, optimized assay α was used to compare three replicate circular or linear pSP64-Adh DNAs (six samples total) at ~ 100 copies/panel. dPCR estimated targets were compared using a two-tailed Student's *t* test. Both linear and circular pSP64-Adh DNA samples were diluted in a constant carrier of 50 ng/ μL sonicated salmon sperm DNA (Agilent) in $1\times$ TE (pH 8).

The Effect of Preamplification on Assay Bias. Linearized pSP64-Adh DNA template diluted to ~ 100 copies/panel either did or did not undergo preamplification treatment using TaqMan PreAmp Master Mix (ABI). Multiplex preamplification included ADH assays α , β , and δ . Preamplified neat product was subjected to a range of dilutions and assessed primarily by qPCR on the Prism 7900 HT real-time PCR platform (ABI) to establish approximate concentration before being transferred to the Biomark system. A dilution (1:325 of neat preamplified product) was chosen for assessment by dPCR due to its close alignment with nonpreamplified target concentration. Each sample type (preamplified and nonpreamplified ADH) was evaluated using three replicate 12.765 chip panels for each of the three assays α , β , and δ , along with NTCs, also assessed with each of the three assays α , β , and δ . All samples were randomized over three 12.765 dPCR chips, with NTCs on each. dPCR estimated targets were compared using a Kruskal–Wallis test. Linear pSP64-Adh DNA samples were diluted to ~ 100 copies/panel in a constant carrier of 50 ng/ μL sonicated salmon sperm DNA (Agilent) in $1\times$ TE (pH 8). All subsequent dilutions of both preamplified (neat) and nonpreamplified samples were made in 0.5% Tween 20 (Sigma). No template controls were performed by adding water in place of template, and all resulted in no signal.

RESULTS AND DISCUSSION

In this study, we evaluated the quantification of low quantities of DNA molecules by dPCR. Although estimated copies based on an absolute count of molecules is the defined measurement unit used for this methodology, we have additionally compared

dPCR estimated targets with the Cq output (more commonly used in conventional qPCR) produced by the Fluidigm Biomark instrument when performing dPCR to establish if there is any association between Cq and dPCR estimated copies. Furthermore, for the experiment investigating dPCR measurement capability for small amounts of DNA (Figure 2), qPCR measurements using the Prism 7900 HT real-time PCR platform (ABI) were made alongside dPCR studies for comparison, measuring the same template.

Quantification of Small Amounts of DNA. We initially investigated the variation in dPCR measurement of reduced quantities of a BCR-ABL DNA standard and the impact of including a cDNA carrier (from wild type HCC1954BL cell line). qPCR measurements were made alongside dPCR studies for comparison. The precision of quantification of the low copy-number linear target was investigated using the 12.765 dPCR chip format with a BCR-ABL assay (Figure 2A–C) and qPCR (Figure 2D–F).

Both technologies showed a linear relationship across the dilutions series from 16 to 128 copies. The data suggested that the presence of carrier improved the sensitivity of both technologies when measuring the two-copy dilution (Supporting Information Figure 2A–B). The mean dPCR estimated target values show good agreement between replicate dilutions, independent of the inclusion of carrier, with no significant difference at the 95% confidence level, $p = 0.80$ (Figure 2A). There was no significant interexperiment variation among the three separate analyses conducted over a period of ~ 5 months (Figure 2A and Table 3), demonstrating high reproducibility. qPCR showed considerably higher interexperimental variation (Figure 2F) and, unlike dPCR, showed improved precision with the inclusion of carrier (Supporting Information Table 2).

dPCR estimated targets for the number of copies/panel was approximately 50% lower than the number of target copies reported by the supplier and was independent of the inclusion of carrier or experiment (Supporting Information Table 3). The qPCR estimated targets did not differ from that generated by UV spectrophotometry (as quoted by the manufacturer). However, this would be expected because the standard curve approach used for quantification was itself defined by UV spectrophotometry. Conversely, dPCR quantification estimates are generated by a count of amplified targets and are independent of any calibration/standard material and associated bias. The precision of both platforms is shown to be high, although dPCR is the more precise of the two technologies.

Data from each platform were used to estimate expanded uncertainty (95% confidence interval calculations, outlined in Supporting Information). qPCR estimates for the 16-copy sample were between 7 and 15 and between 11 and 22 copies/reaction with and without carrier, respectively, whereas for the 128-copy sample, they were between 78 and 147 copies/reaction, both with and without carrier. Alternatively, dPCR expanded uncertainty estimates for 16 copies were between 5 and 9 copies/panel, and for 128 copies, between 52 and 78 copies/panel, with no difference reported for carrier inclusion. A notable benefit of dPCR over qPCR is that this analysis technique requires no standard, calibration, or information about the molecular weight distribution of the template molecules.¹⁴ This enables an absolute value to be assigned of amplifiable DNA target, which we show here can be highly reproducible.

Quantification cycle (Cq, formerly threshold cycle Ct or crossing point C_p^{23}) data from the 128 copies/panel (dPCR)

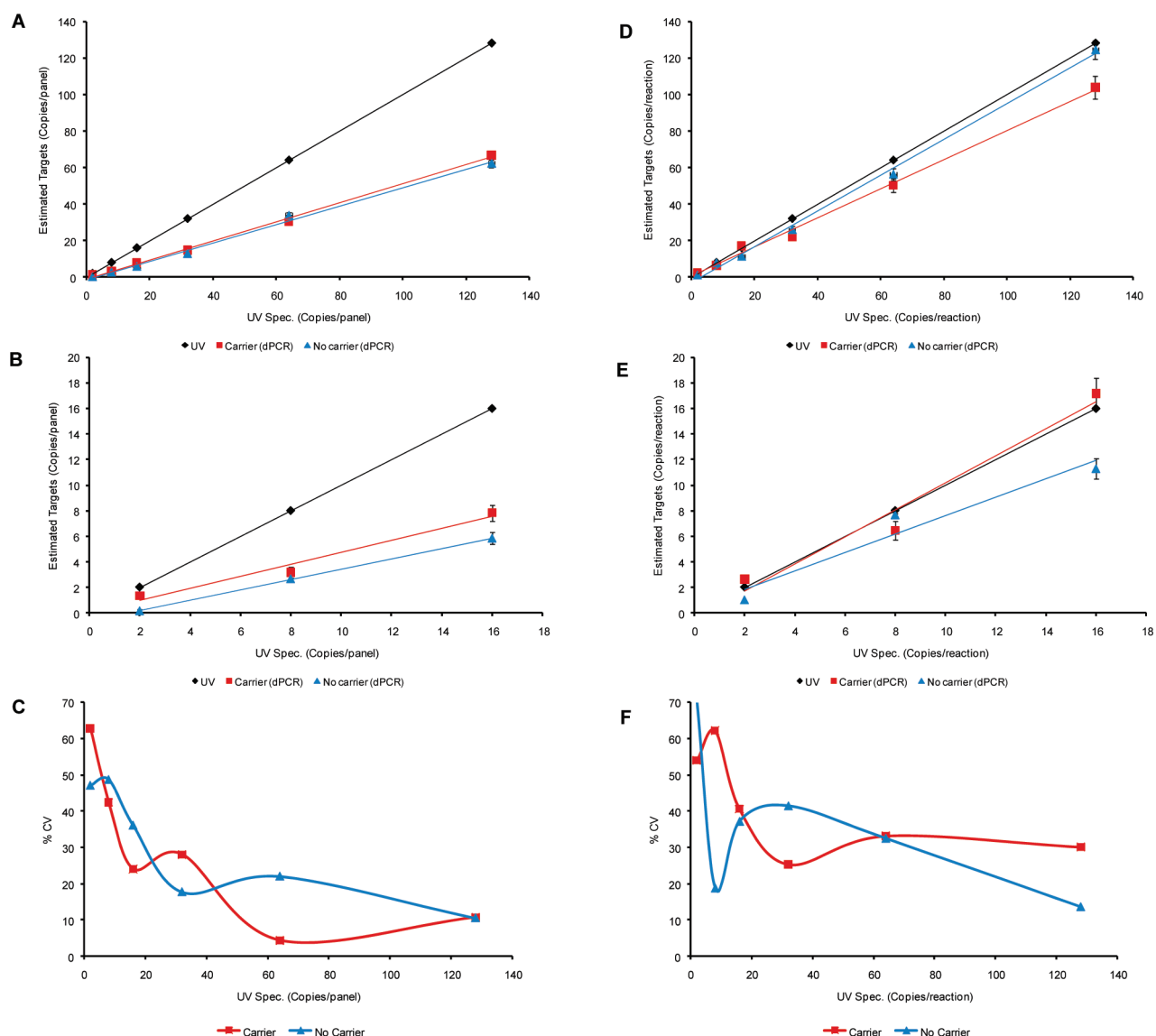


Figure 2. Microfluidic dPCR versus conventional qPCR quantification. BCR-ABL Mbc standards were diluted to approximately 2, 8, 16, 32, 64, or 128 copies/panel (based on manufacturer's quoted quantification). Samples were either spiked into a background of total human cDNA (carrier), or water (no carrier). Error bars given as standard error, $n = 3$. (A) dPCR estimated targets are plotted against expected copy number (generated following dilution of DNA solution originally quantified by UV spectrophotometry). Analysis performed using the Biomark system (Fluidigm). (B) Extended lower range, 2–16 copies, of data plotted in A. (C) Analysis of precision when dilutions are performed with and without carrier. (D) qPCR estimated targets are plotted against expected copy number (as for dPCR). Analysis performed using the Prism 7900 HT real-time PCR system (ABI). (E) Extended lower range, 2–16 copies, of data plotted in D. (F) Precision analysis of carrier and no carrier dilutions.

Table 3. Summary of ADH Estimated Quantity Using Nanodrop UV Spectrophotometry and dPCR

experiment		UV estimate copies/panel	dPCR estimate copies/panel (n^a)	dPCR % CV	p value ^b
ADH: 3 assays, 1 digest ^c	assay α	~100	159 (3)	9.57	0.02
	assay β		159 (3)	7.67	0.01
	assay δ		160 (3)	5.45	0.01
ADH: 1 assay, 3 digests ^c	linear	~57	91 (3)	32.15	0.20
	circular		20 (3)	38.84	0.02

^a Number of replicate panels per observation. ^b Two-sample Student's t test used to compare nanodrop UV spectrophotometry with dPCR estimated target copy number. ^c Both ADH experiments were performed in carrier (50 ng/ μ L salmon sperm DNA).

or copies/reaction (qPCR) were compared between carrier and no carrier samples from three respective independent

experiments (Figure 3A and B). Although there was no significant difference between carrier and no carrier sample quantification by

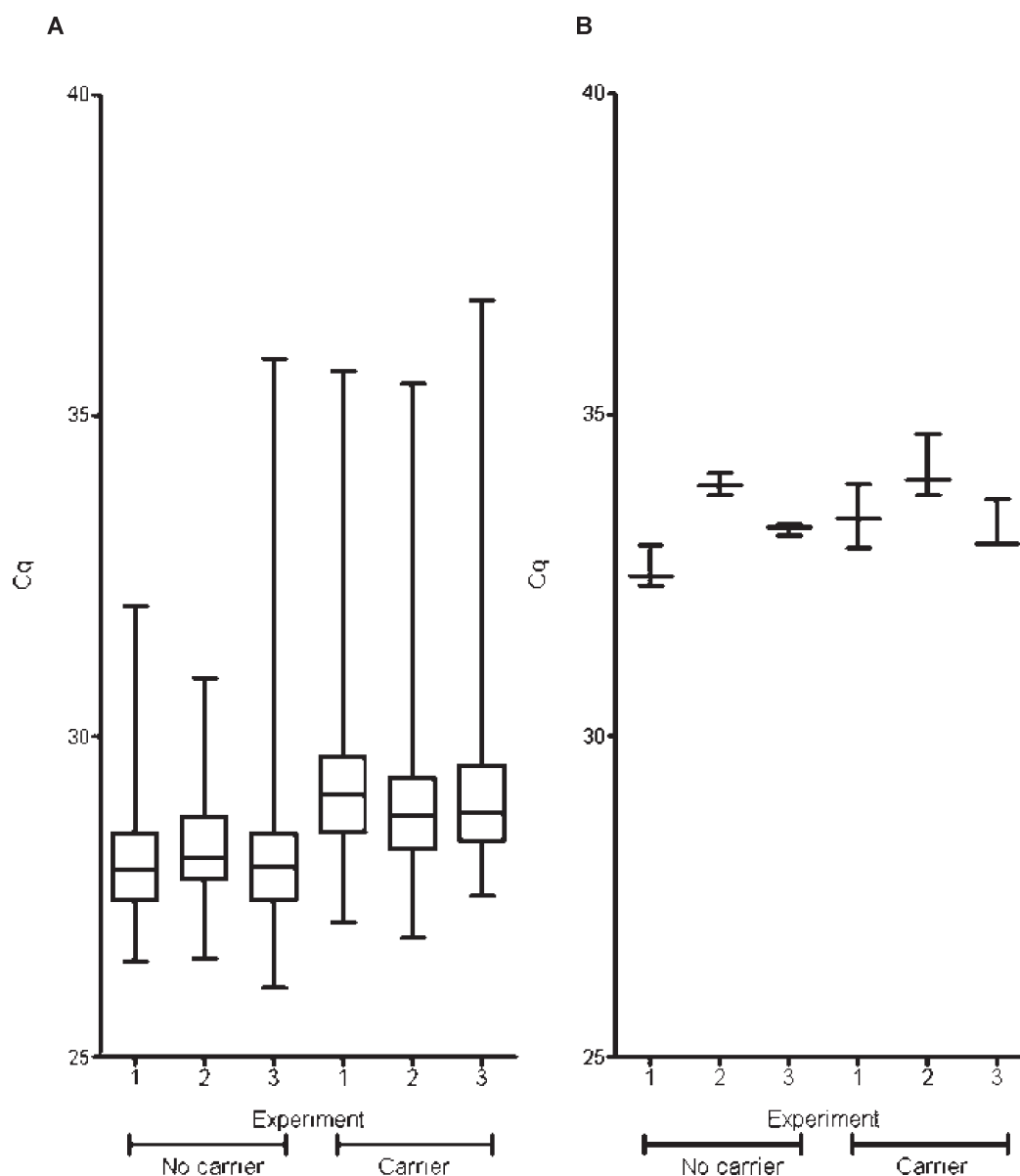


Figure 3. Impact of carrier on dPCR and qPCR quantification. Cq data (BCR-ABL Mbc standard) from the 128-copy dilution are plotted as carrier (total human cDNA) versus no carrier samples to show the data spread for the three replicate dPCR (A) and qPCR (B) experiments. Box and whisker plots depict the observational range, lower quartile (25th percentile), upper quartile (75th percentile), and median.

dPCR (Supporting Information Table 3), the Cq data of carrier versus no carrier samples were significantly different at the 99.99% confidence interval, $p < 0.0001$ (pooled replicate positive chambers, using the Mann–Whitney U test), with the presence of carrier resulting in an increase in the median Cq of 0.89. In addition, the data indicate the impact of chip-to-chip (run-to-run) differences on Cq when the same fluorescence threshold was used (Figure 3A). Similar observations were made using the qPCR 7900 platform, which therefore impacted on the measurement result. Again, although there was no interexperiment variation in dPCR estimated targets, the Cq differences were significant at the 95% level (using the Kruskal–Wallis test, separate tests for carrier, $p < 0.05$; and no carrier, $p < 0.003$). When the interexperimental qPCR results were compared in the same way, only noninclusion of carrier resulted in a significant difference from UV spectrophotometry quantification ($p < 0.03$).

An underlying factor explaining the dPCR observations may be due to use of normal human carrier cDNA, which was chosen to mimic real clinical samples, binding some of the primers and, thus, delaying amplification. This, combined with the single copy partitioning intrinsic to dPCR, might explain why increased Cq was observed with dPCR but not when performing qPCR. In addition to the usual quenching of reagent availability observed when using carrier in samples, the primers may bind to the target sequence in the wild-type BCR and ABL genes, as well as nonspecific binding throughout the genome. This could cause an initial reduced availability of primers that may explain this observation.

Another observation was that the Cq spread was considerably greater when performing dPCR than the corresponding qPCR data (Figure 3). This is linked to the fact that dPCR is performing a series of single (or near single)-copy PCR reactions. qPCR variability increases as copy number decreases,²⁴ which is directly

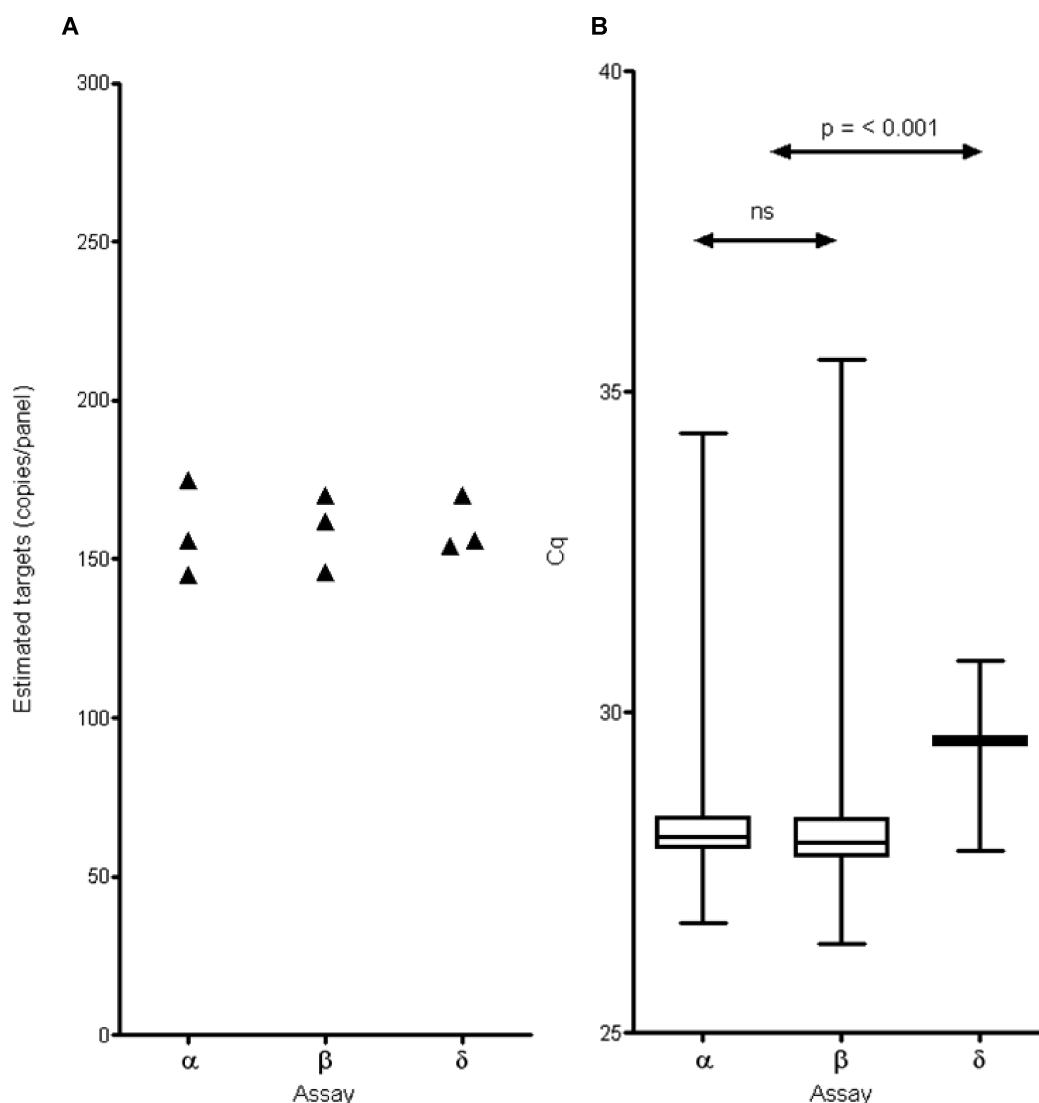


Figure 4. dPCR assay comparability. Three different assays were employed to analyze the same linearized ADH template by dPCR. Each sample consisted of ~ 100 copies/panel estimated using Nanodrop UV spectrophotometry. (A) Estimated targets and (B) Cq data.

linked to increased Cq variability. The main observations were that, although Cq data and spread can vary with the addition of carrier and with the use of different chips, this had no influence on the actual dPCR estimated targets when using this assay and template (Table 3). This finding suggests dPCR has huge potential for accurate absolute molecular quantification because it does not depend upon a standard curve, which adds another level of complexity when comparing results between different laboratories.

The Effect of Different dPCR Assays on dPCR Measurements. In the next experiment, we assessed the impact of using different PCR assays, targeting distinct regions of the same linearized ADH plasmid molecule, on the estimated targets reported by dPCR (Figure 4A and 4B). The PCR reactions were optimized using the Prism 7900 HT real-time PCR system (ABI),¹⁶ exhibiting efficiencies of $\geq 96\%$.

All three assays reported higher quantities by dPCR than estimated using Nanodrop UV spectrophotometry (Table 3; ADH: 3 assays, 1 digest), with all three significant at the 95% confidence interval (average $p = 0.04$). When Cq data (with all assays measured at the same fluorescence threshold) are plotted

to compare the three different reactions, the median Cq and variation were comparable between assays α and β , but the δ assay had less variation and a different median Cq (data evaluated using the Kruskal–Wallis test followed by Dunn’s multiple comparison test, Figure 4B). Despite these qPCR observations, each assay produced highly consistent dPCR quantification of the estimated targets, with no significant difference between assays ($p = 0.93$ using the Kruskal–Wallis test) (Figure 4A).

It is important to note that all three assays were optimized to be highly efficient by qPCR (96–100%). Whereas PCR efficiency is likely to play an important role in absolute quantification,¹⁶ it has been suggested that dPCR is less dependent on assay efficiency for quantification due to the underlying principle of single molecule amplification.²⁵ Our findings suggest that dPCR is reproducible between different optimized assays. This is comparable to the investigations of Bhat et al.²⁶ at higher concentrations of DNA.

The Effect of Linear versus Circular Supercoiled Molecules on dPCR Measurements. An investigation of the impact of circular versus linear DNA template was also performed using

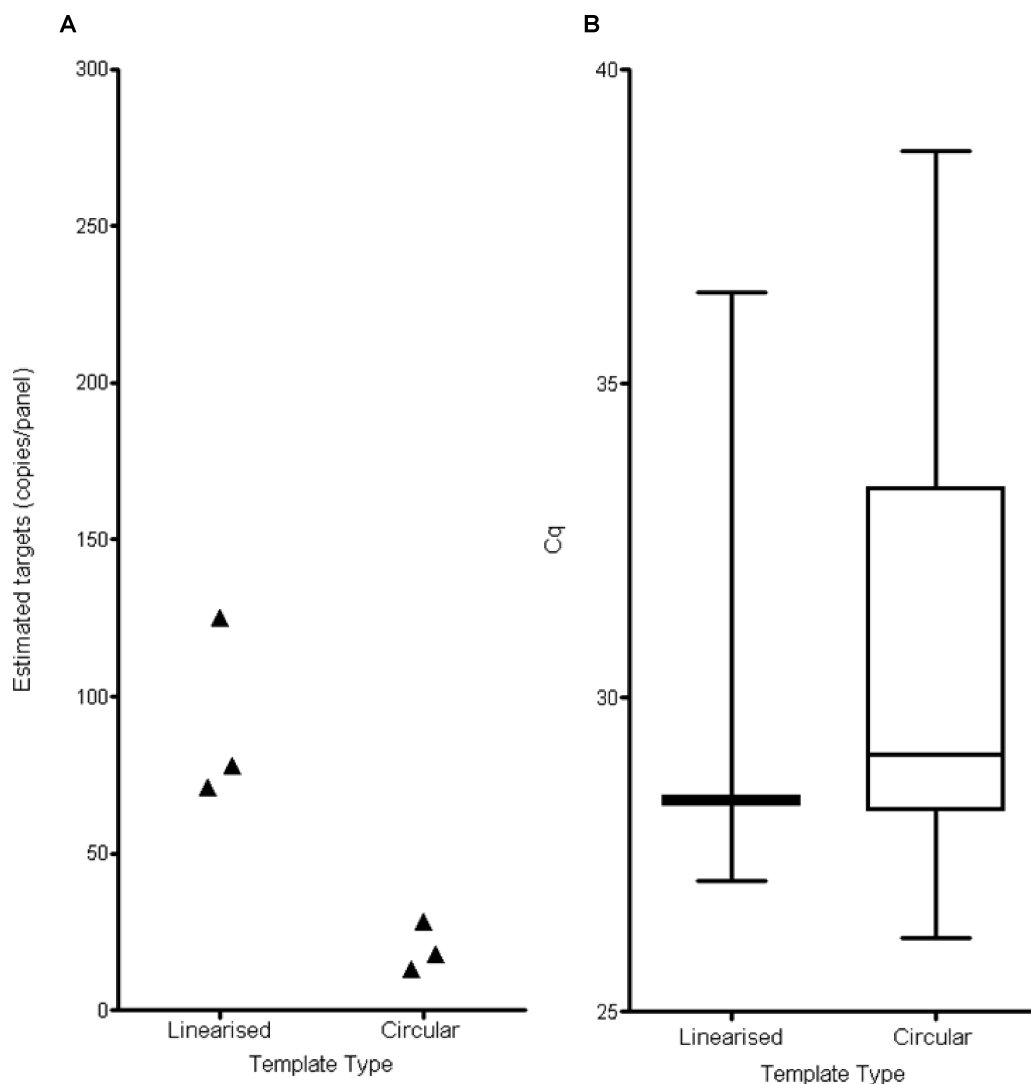


Figure 5. dPCR quantification of circularized versus linearized plasmid. Three replicate samples (~ 57 copies/panel) of both circularized plasmid and linearized plasmid containing an ADH insert were analyzed by microfluidic dPCR. (A) Estimated targets and (B) Cq data using a single assay to analyze three linearized and three circular templates.

microfluidic dPCR (Figure 5). It has previously been demonstrated that the type of template can affect quantification values when using qPCR.^{12,26–28} DNA fragmentation or plasmid linearization can increase amplification efficiency and minimize bias in estimation of the true copy number.^{12,26–31} In the experiment described here, directly comparable aliquots of ADH template were evaluated in both circular and linearized forms. The same eluate was either digested ($n = 3$ reactions) or undigested ($n = 3$ negative control digest reactions) prior to dilution to ~ 57 copies/panel, based on Nanodrop UV spectrophotometry estimations.

These data show that DNA template type affected the dPCR estimated targets and resulting Cq data obtained (Figure 5A and B). Circularized plasmid exhibited lower estimated targets than predicted using Nanodrop UV spectrophotometry ($p = 0.02$, Table 3), whereas linearized plasmid average estimated targets were in agreement with UV spectrophotometry estimates ($p = 0.20$, Table 3). We also found that the Cq data was template-structure-dependent, with a particularly large variation in Cq values, from 26.2 to 38.7, for circularized template (Figure 5B), which was not observed with the linear template.

Consequently, in this experiment, both the Cq and dPCR estimated targets were affected by the structure of the template. This leads to the question of why these discrepancies occur. An observation that may allude to these differences is the increased Cq variability observed for circular template. The underlying assumption associated when performing dPCR is that the presence of a template molecule will lead to measurable signal. Nevertheless, the increased Cq variation observed when investigating circular template, combined with the single molecule per chamber methodology of dPCR, suggest some reactions may be delayed in initiation or have reduced amplification efficiency. It is possible that in extreme cases, this delay may manifest as no amplification and, hence, underestimation of target concentration. When performing dPCR, this cannot be explained by mixed amounts of different template types (such as variable amounts of nicked open circle plasmids) that may explain similar results when performing qPCR because the vast majority of the individual dPCR reactions are performed on a single template molecule.

Another possible explanation for discrepancies in dPCR quantification is that linear template has the potential to be

present in both double stranded (ds) or denatured single stranded (ss) forms. It is therefore possible for one dsDNA molecule to populate two individual dPCR reactions. Consequently, the measurement of DNA by dPCR has the potential to differ by as much as 2-fold depending on the level of sample denaturation. Although circular DNA can be denatured, the supercoiled nature of the plasmid prevents the resultant single strands from being separated and populating different individual dPCR reactions. As such, no overestimation of quantity is likely for circular template as a result of denaturation. Further work is required to elucidate the discrepancies between platform quantification, but it is also important to recognize that results obtained using different template types or preparations should not be directly compared without suitable supportive evidence.

The Effect of Pre-amplification on Assay Bias. Another notable benefit of dPCR over qPCR, which we demonstrate above and has previously been described,¹⁴ is improved measurement precision. As such, assessments of linearity and measurement bias are afforded better resolution. We utilized this capability to investigate the impact of pre-amplification on dPCR interassay evaluation of comparative results while continuing to investigate low copy-number quantification. Pre-amplification is an increasingly necessary method for assisting in the quantification of nucleic acid samples that have limited amounts of material. The underlying assumption is that any intertarget bias introduced by pre-amplification is negligible, and the pre-amplified sample has essentially the same proportion of targets of interest as the sample prior to the pre-amplification step. This assumption is particularly important when relative copy numbers are being assessed, (e.g., for gene expression analysis) or when accurate absolute quantification or copy number variation analysis is required, (e.g., for diagnosis of disease).

To test this, we analyzed the same ADH molecule with the three assays described above, before and after pre-amplification, to ascertain potential bias introduced specifically by the pre-amplification process (Figure 6). Following pre-amplification of target, samples were diluted to within range of nonpre-amplified sample concentrations to facilitate direct comparison and to maintain our primary objective: analyzing low-concentration samples (≤ 200 copies/panel). Figure 6 showed little variation in estimated targets between all three assays for nonpre-amplified target, and there was no significant difference at the 95% confidence interval ($p = 0.37$), in agreement with our previous observations. However, there was a significant difference observed in estimated targets between assays for the pre-amplified sample ($p < 0.03$).

Our findings are in disagreement with previously published data using delta delta ($\Delta\Delta$) Cq analysis methods for multiplex pre-amplification of individual target molecules, which suggested that no experimental bias was introduced.^{32,33} However, unlike our investigation, the experimental plan for both studies did not consider assay-specific amplification bias within nonpre-amplified samples and, as such, is open to different interpretation. Furthermore, although little or no pre-amplification bias may have been observed when measuring low amounts of cDNA by qPCR, our contrasting data suggests that dPCR has increased sensitivity for this application: the largest reported bias introduced by pre-amplification, between the β and δ assays, was ~ 2 -fold. On this basis, we would therefore argue that dPCR may be the only methodology sensitive enough to discern subtleties in pre-amplification bias. In our study, with this template and assay trio, we have established that pre-amplification of target can introduce

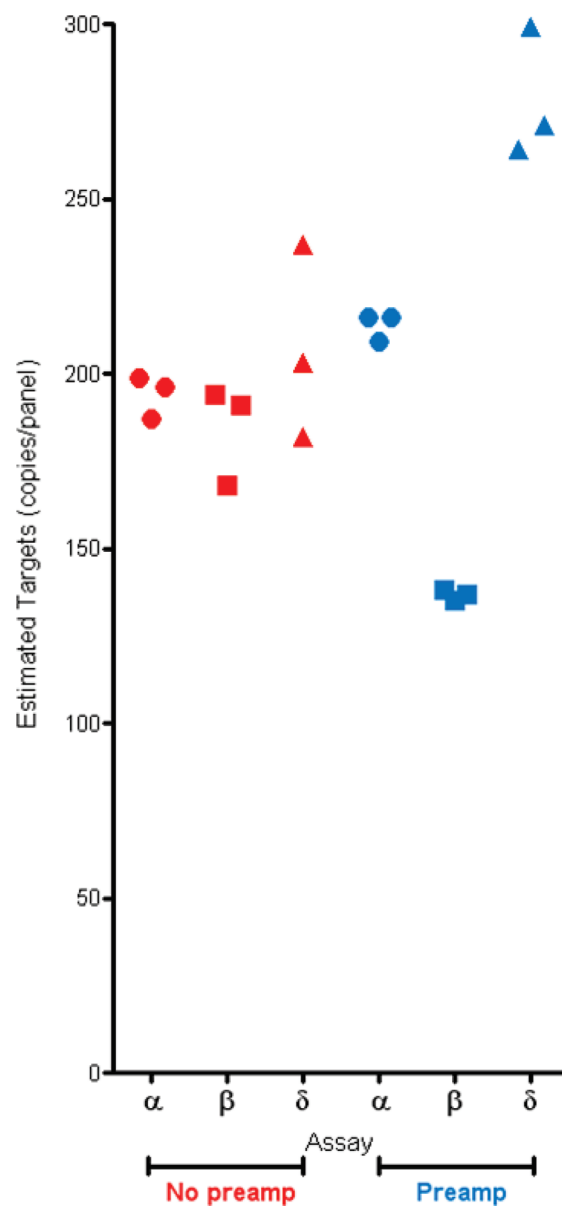


Figure 6. dPCR quantification of pre-amplified versus nonpre-amplified target. One aliquot of linearized pSP64-Adh DNA template diluted to ~ 100 copies/panel was subjected to pre-amplification before dPCR analysis. Pre-amplified product was diluted to within concentration range of nonpre-amplified sample. For both samples, three replicate 12.765 dPCR panels were evaluated using each of the three distinct ADH assays: α , β , and δ . Red data points, no pre-amplification; blue data points, pre-amplification. \bullet , ADH assay α ; \blacksquare , ADH assay β ; \blacktriangle , ADH assay δ .

significant experimental bias. If consistency in assay-specific bias is maintained across different pre-amplification replicates, then normalization of data may be performed to alleviate this bias.

One important additional finding when comparing all the above experiments was the frequent divergence in observed difference between Nanodrop UV spectrophotometry and dPCR quantification, as evidenced by the appropriate p values (Table 3). This type of disparity has also been observed in previous studies.³⁴ UV spectrophotometry is an established method for measuring nucleic acids; however, common contaminants of DNA extracts, such as proteins, RNA, and salts, can increase the

spectrophotometric estimation of DNA concentration. UV spectrophotometry cannot distinguish between single-stranded DNA and double-stranded DNA in solution or between target DNA and other potentially contaminating sources of DNA or RNA. In addition, UV spectrophotometry cannot indicate the ability of PCR to successfully amplify a DNA sample.³⁵ Thus, this method has limitations that may contribute to inaccuracy of DNA concentration estimates.

dPCR is based on the principle that an absolute count of amplified targets can be achieved, unlike conventional qPCR, which provides a relative quantification and, as such, is intrinsically linked to the original quantification technique, often UV spectrophotometry. dPCR works on the premise that every molecule of target is successfully amplified in dPCR analysis, and therefore, dPCR should, in theory, provide the most accurate method of molecular quantification. However, this assumption must be made with caution. Although our findings demonstrate dPCR can be both precise and highly reproducible, the fact that different templates can give differing results suggests further work is required before the nature of the absolute measurement can be fully defined. To that end, validation of a suitable certified reference material specifically generated to target the question of absolute quantification by dPCR would be indispensable.

CONCLUSIONS

The findings of this study provide a range of information on the utility of dPCR for low copy molecular measurement. We demonstrate that dPCR can be highly reproducible when performed at different times, when different primer sets are targeting the same molecule, and when carrier is included. In this study dPCR exhibited good biological sensitivity and was reproducible outside the range recommended by the instrument manufacturer, detecting 16 estimated targets with high precision. Differing dPCR estimated targets could be generated when using different template types and when comparing dPCR quantification with Nanodrop UV spectrophotometry. Consequently, when comparing data, experimental consistency is essential. The origin of these discrepancies is yet to be defined, and therefore, further work is required before dPCR can be classified fundamentally as an absolute quantification technique. It is also important to note that for the experimental system studied here, preamplification of target introduces assay-specific bias, and we therefore recommend that before applying preamplification techniques to sample unknowns, validation of preamplification on an assay-specific basis should be performed as standard. These data presented here demonstrate that dPCR can offer a highly sensitive, precise, and reproducible method for molecular quantification of small amounts of DNA.

ASSOCIATED CONTENT

S Supporting Information. Additional information as noted in text. This material is available free of charge via the Internet at <http://pubs.acs.org>.

AUTHOR INFORMATION

Corresponding Author

*Phone: +44 (0)20 8943 7655. Fax: +44 (0)20 8943 2767. E-mail: jim.huggett@lgc.co.uk

Author Contributions

C.A.F. conceived the project and assisted with experimental design. R.S., J.F.H., and D.J.S. designed the specific experiments. R.S. and C.A.B. conducted the practical experimentation. R.S., J.F.H., and C.A.B. evaluated results and interpreted the data. R.S., J.F.H., and D.J.S. wrote the manuscript. All authors approved the final manuscript.

Notes

The authors confirm no financial or nonfinancial competing interests.

ACKNOWLEDGMENT

We thank Drs. Ellison and Minguez for their assistance during statistical analysis. The work described in this manuscript was funded by the UK National Measurement System.

REFERENCES

- (1) Vogelstein, B.; Kinzler, K. W. *Proc. Natl. Acad. Sci. U.S.A.* **1999**, *96*, 9236–9241.
- (2) Shih, I. M.; Yan, H.; Speyrer, D.; Shmookler, B. M.; Sugarbaker, P. H.; Ronnett, B. M. *Am. J. Surg. Pathol.* **2001**, *25*, 1095–1099.
- (3) Shih, I. M.; Zhou, W.; Goodman, S. N.; Lengauer, C.; Kinzler, K. W.; Vogelstein, B. *Cancer Res.* **2001**, *61*, 818–822.
- (4) Singer, G.; Kurman, R. J.; Chang, H. W.; Cho, S. K.; Shih, I. M. *Am. J. Pathol.* **2002**, *160*, 1223–1228.
- (5) Zhou, W.; Galizia, G.; Lieto, E.; Goodman, S. N.; Romans, K. E.; Kinzler, K. W.; Vogelstein, B.; Choti, M. A.; Montgomery, E. A. *Nat. Biotechnol.* **2001**, *19*, 78–81.
- (6) Zhou, W.; Goodman, S. N.; Galizia, G.; Lieto, E.; Ferraraccio, F.; Pignatelli, C.; Purdie, C. A.; Piris, J.; Morris, R.; Harrison, D. J.; Paty, P. B.; Culliford, A.; Romans, K. E.; Montgomery, E. A.; Choti, M. A.; Kinzler, K. W.; Vogelstein, B. *Lancet* **2002**, *359*, 219–225.
- (7) Fan, H. C.; Quake, S. R. *Anal. Chem.* **2007**, *79*, 7576–7579.
- (8) Lo, Y. M.; Lun, F. M.; Chan, K. C.; Tsui, N. B.; Chong, K. C.; Lau, T. K.; Leung, T. Y.; Zee, B. C.; Cantor, C. R.; Chiu, R. W. *Proc. Natl. Acad. Sci. U.S.A.* **2007**, *104*, 13116–13121.
- (9) Zimmermann, B. G.; Grill, S.; Holzgreve, W.; Zhong, X. Y.; Jackson, L. G.; Hahn, S. *Prenatal Diagn.* **2008**, *28*, 1087–1093.
- (10) Ottesen, E. A.; Hong, J. W.; Quake, S. R.; Leadbetter, J. R. *Science* **2006**, *314*, 1464–1467.
- (11) Warren, L.; Bryder, D.; Weissman, I. L.; Quake, S. R. *Proc. Natl. Acad. Sci. U.S.A.* **2006**, *103*, 17807–17812.
- (12) Burns, M. J.; Burrell, A. M.; Foy, C. A. *Eur. Food Res. Technol.* **2010**, *231*, 353–362.
- (13) Corbisier, P.; Bhat, S.; Partis, L.; Xie, V. R.; Emslie, K. R. *Anal. Bioanal. Chem.* **2010**, *396*, 2143–2150.
- (14) White, R. A., 3rd; Blainey, P. C.; Fan, H. C.; Quake, S. R. *BMC Genomics* **2009**, *10*, 116.
- (15) BioMark Advanced Development Protocol 10. Absolute quantitation using the digital array; Fluidigm (Fluidigm Corporation, S.F.).
- (16) Dhanasekaran, S.; Doherty, T. M.; Kenneth, J. *J. Immunol. Methods* **2010**, *354*, 34–39.
- (17) Anderson, M.; Burrell, A.; Barbagallo, R.; Foy, C. *MFB (2004–2007) programme*; 2006; pp 1–10.
- (18) Beillard, E.; Pallisgaard, N.; van der Velden, V. H.; Bi, W.; Dee, R.; van der Schoot, E.; Delabesse, E.; Macintyre, E.; Gottardi, E.; Saglio, G.; Watzinger, F.; Lion, T.; van Dongen, J. J.; Hokland, P.; Gabert, J. *Leukemia* **2003**, *17*, 2474–2486.
- (19) Gabert, J.; Beillard, E.; van der Velden, V. H.; Bi, W.; Grimwade, D.; Pallisgaard, N.; Barbany, G.; Cazzaniga, G.; Cayuela, J. M.; Cave, H.; Pane, F.; Aerts, J. L.; De Micheli, D.; Thirion, X.; Pradel, V.; González, M.; Viehmann, S.; Malec, M.; Saglio, G.; van Dongen, J. J. *Leukemia* **2003**, *17*, 2318–2357.

- (20) Qin, J.; Jones, R. C.; Ramakrishnan, R. *Nucleic Acids Res.* **2008**, *36*, e116.
- (21) Dube, S.; Qin, J.; Ramakrishnan, R. *PLoS One* **2008**, *3*, e2876.
- (22) Warren L. A.; Weinstein J. A.; Quake S. R. . Ph.D. Thesis (Appendix, p188), California Institute of Technology, 2007.
- (23) Bustin, S. A.; Benes, V.; Garson, J. A.; Hellemans, J.; Huggett, J.; Kubista, M.; Mueller, R.; Nolan, T.; Pfaffl, M. W.; Shipley, G. L.; Vandesompele, J.; Wittwer, C. T.; *Clin. Chem.* **2009**, *55*, 611–622.
- (24) Huggett, J. F.; Taylor, M. S.; Kocjan, G.; Evans, H. E.; Morris-Jones, S.; Gant, V.; Novak, T.; Costello, A. M.; Zumla, A.; Miller, R. F. *Thorax* **2008**, *63*, 154–159.
- (25) Weaver, S.; Dube, S.; Mir, A.; Qin, J.; Sun, G.; Ramakrishnan, R.; Jones, R. C.; Livak, K. J. *Methods* **2010**, *40*, 271–276.
- (26) Bhat, S.; Curach, N.; Mostyn, T.; Bains, G. S.; Griffiths, K. R.; Emslie, K. R. *Anal. Chem.* **2010**, *82*, 7185–7192.
- (27) Chen, J.; Kadlubar, F. F.; Chen, J. Z. *Nucleic Acids Res.* **2007**, *35*, 1377–1388.
- (28) Hou, Y.; Zhang, H.; Miranda, L.; Lin, S. *PLoS One* **2010**, *5*, e9545.
- (29) Bhat, S.; Herrmann, J.; Armishaw, P.; Corbisier, P.; Emslie, K. R. *Anal. Bioanal. Chem.* **2009**, *394*, 457–467.
- (30) Bhat, S.; McLaughlin, J. L.; Emslie, K. R. *Analyst* **2010**, *136*, 724–732.
- (31) Vazquez, R.; Steinberg, M. L. *Biotechniques* **1999**, *26*, 91–95.
- (32) Noutsias, M.; Rohde, M.; Block, A.; Klippert, K.; Lettau, O.; Blunert, K.; Hummel, M.; Kuhl, U.; Lehmkuhl, H.; Hetzer, R.; Rauch, U.; Poller, W.; Pauschinger, M.; Schultheiss, H. P.; Volk, H. D.; Kotsch, K. *BMC Mol. Biol.* **2008**, *9*, 3.
- (33) Stanley, S.; Lee, C.; Wilde, J.; Coudry, R.; Spittle, C.; Stevens, J. TaqMan PreAmp Master Mix Kit for Real-Time Gene Expression Analysis with Sample Limited Specimens.
- (34) Oehler, V. G.; Qin, J.; Ramakrishnan, R.; Facer, G.; Ananthnarayan, S.; Cummings, C.; Deininger, M.; Shah, N.; McCormick, F.; Willis, S.; Daridon, A.; Unger, M.; Radich, J. P. *Leukemia* **2009**, *23*, 396–399.
- (35) Haque, K. A.; Pfeiffer, R. M.; Beerman, M. B.; Struewing, J. P.; Chanock, S. J.; Bergen, A. W. *BMC Biotechnol.* **2003**, *3*, 20.